Developmental Biology 450 (2019) 90–100

Contents lists available at ScienceDirect

Developmental Biology

journal homepage: www.elsevier.com/locate/developmentalbiology

miR-29c regulates neurogliogenesis in the mammalian retina through REST

Xiaohuan Xia, Pooja Teotia, Iqbal Ahmad *

Department of Ophthalmology and Visual Science, University of Nebraska Medical Center, Omaha, NE, 68198, USA

ARTICLE INFO

Keywords:
miR-29
REST
Neurogliogenesis
Retina
microRNA
Differentiation

ABSTRACT

In the developing central nervous system, including its simple and accessible model retina, neurogenesis is followed by gliogenesis. However, the mechanism underlying the neurogliogenic switch remains poorly understood despite the identification of several regulatory genes, associated with the lineage identity and transition. The mechanism may involve cross talks between regulatory genes, facilitated through microRNAs. Here, we posit *miR-29c* as one of the regulatory miRNAs that may influence neuronal versus glial differentiation. We observed that the temporal patterns of *miR-29c* expression corresponded with late retinal histogenesis, the stage in the developing retina when neurogliogenic decision predominantly occurs. Examination of the effects of *miR-29c* on neurogliogenesis by the perturbation of function approach revealed that *miR-29c* preferentially facilitated differentiation of late RPCs into rod photoreceptors and bipolar cells, the late-born neurons, at the expense of Müller glia, the sole glia generated by retinal progenitor cells. We further observed that *miR-29c* facilitated neurogenesis and inhibited gliogenesis by regulating the expression of *RE-1 silencing transcription factor* (*REST*), which encodes a transcriptional repressor of cell cycle regulators and neuronal genes. Thus, *miR-29c* may influence neurogliogenic decision in the developing retina by regulating the instructive out put of a molecular axis helmed by REST.

1. Introduction

MicroRNAs (miRNAs) are short non-coding antisense RNAs that silence the expression of specific mRNAs either by promoting their degradation or interfering with their translation (Ebert and Sharp, 2012). Therefore, miRNAs represent an additional regulatory mechanism for contextual fine-tuning of the hierarchical gene expression required for the stage-specific generation of cell types in complex tissues like the central nervous system (CNS). We are testing this premise in the mammalian retina, a simple and accessible CNS model. The retina consists of seven different cell types that are generated by the multipotential retinal progenitor cells (RPCs) in an evolutionarily conserved temporal sequence, spanning two distinct stages of histogenesis (Rapaport et al., 2004; Young, 1985). As a general rule, retinal ganglion cells (RGCs), horizontal cells (HCs), cone photoreceptors (CPs), and amacrine cells (ACs) are born during early histogenesis, while rod photoreceptors (RPs), bipolar cells (BCs), and Müller glia (MG) are born during late histogenesis (Rapaport et al., 2004; Young, 1985).

Evidence has emerged that miRNAs are involved in retinal histogenesis. For example, a global stage-specific loss of miRNAs through Cre-mediated excision of *Dicer*, which encodes the enzyme involved in the biogenesis of miRNA, disrupted retinal development (Iida et al., 2011), while it's lack of function in late RPCs resulted in retinal disorganization (Damiani et al., 2008). Subsequent studies revealed the role of specific miRNAs and their regulators in retinal development. For example, the hetrochronic miRNA, *let-7* was observed to be involved in the temporal progression of RPCs, required for the stage-specific retinal histogenesis (Decembrini et al., 2009; La Torre et al., 2013). Recently it was demonstrated that *let-7* promoted RPC differentiation, regardless of neuronal and glial lineage, by shifting the balance from RPC maintenance to their differentiation during late histogenesis (Xia and Ahmad, 2016a). That *let-7* may not be involved in cell-type specific differentiation in the retina was further demonstrated when it was observed not to be a part of the regulatory axis defined by Lin28a, a heterochronic gene that promoted differentiation in favor of neurons versus glia during late histogenesis (Xia et al., 2018).

These observations suggested the involvement of additional temporally expressed miRNAs that modulate cell-type specific gene expression for differentiation of RPCs along different sub-lineages. To identify such miRNAs we examined their involvement in late histogenesis when RPCs differentiate into either neurons (RPs and BCs) or glia (MG). Here, screening of developmentally expressed miRNAs using the microarray

* Corresponding author. Department of Ophthalmology and Visual Science, University of Nebraska Medical Center, Durham Research Center 1, Room 4034, 985840 Nebraska Medical Center, Omaha, NE, 68198-5840, USA.
E-mail address: iahmad@unmc.edu (I. Ahmad).

https://doi.org/10.1016/j.ydbio.2019.03.013
Received 3 January 2019; Received in revised form 5 March 2019; Accepted 20 March 2019
Available online 23 March 2019

and functional perturbation analyses we demonstrate that *miR-29c* regulates late RPCs differentiation along neuronal and glial lineages. It facilitates neuronal differentiation over that of glia by silencing RE-1 silencing transcription factor (*REST*), a negative regulator of cell cycle- and neuron-specific genes, and non-neuronal phenotype (Ballas et al., 2005). Our results posit *miR-29c* as one of the regulators of neurogliogenic decision in the developing retina.

2. Materials and methods

This study was approved by the Institutional Animal Care and Use Committee (IACUC) at the University of Nebraska Medical Center (protocols #95-005-09FC and #97-100-08FC). Animals were housed in the Department of Comparative Medicine at the University of Nebraska Medical Center. Timed pregnant Sprague Dawley rats from SASCO and Charles River Laboratories were used to carry out all experiments. Rats were euthanized by CO_2 exposure followed by decapitation using sterile surgical scissors to ensure death.

2.1. Neurosphere assay

Retinas from embryonic day 18 (E18) rats were dissected and dissociated as previously described (Xia and Ahmad, 2016a). Briefly, neurospheres were generated from dissociated E18 retinal cells by culturing for 5 days in RCM (DMEM-F12, N2 supplement, 2 mM L-glutamine, 100 U/ml penicillin, 100 μg/ml streptomycin) and FGF2 (10 ng/ml). On the fifth day, generated neurospheres were collected and transferred to Poly-D-Lysine and laminin coated plates and cover slips. Neurospheres were cultured in RCM:E18 conditioned medium (1:1) supplemented with 2% Knockout Serum (KOS), 1 mM Taurine, 3 μM DAPT, 500 nM retinoic acid, and 15 ng/ml BMP4 for facilitating differentiation. The differentiation was terminated 5 days after plating.

2.2. Viral vectors

The PreMiR-miR-29c (MMIR-29c-PA-1) for *miR-29c* over-expression with control Pre-000 (PMIRH000-PA-1) and miRZip-29c (MZIP29c-PA-1) for *miR-29c* knockdown with control Zip-000 (MZIP000-PA-1) lentivirus constructs were obtained from System Biosciences (Mountain View, CA). The backbone of MMIR-29c-PA-1 and PMIRH000-PA-1 vectors was the dual promoter viral plasmid, PMIRHxxx-PA-1, in which pre-*miR-29c* and *GFP* expression was driven by CMV and EF1 promoters, respectively. The backbone of MZIP29c-PA-1 and MZIP000-PA-1 vectors was the dual promoter viral plasmid, MZIPxxx-PA-1, in which *miR-29c* shRNA and *GFP* expression was driven by H1 and CMV promoters, respectively. The REST siRNA set and its scrambled control was purchased from Applied Biological Materials (Vancouver, Canada). The backbone of REST siRNA and scrambled control vectors was the dual promoter viral plasmid, pGFP-iLenti, in which REST siRNA and *GFP* expression was driven by H1 and CMV promoters, respectively.

2.3. Lentivirus preparation and transduction

Lentivirus preparation and transduction were carried out as previously described (Xia and Ahmad, 2016a). Briefly, the recombination lentiviral particles were generated using the ABM lentivirus packaging system (BC, Canada) through transient transfection of T293 cells. Viral particles were concentrated using BioVision PEG lentivirus precipitation kit (Milpitas, CA). Virus titers were determined using ABM lentivirus titration kit. The retinal dissociates, neurosphere cells, and explants were transduced with lentiviruses with multiplicity of infection (MOI) of 4. Twelve hours after transduction, medium containing virus was replaced by fresh medium. The transduction efficiency was determined 48 h post-transduction by direct observation and sorting of GFP^+ cells. The perturbation experiments were carried out three times in triplicates as follows: 10–14 E18 embryos/group (*in vitro* perturbation) and 9 retinae/group (*ex vivo* perturbation).

2.4. Preparation of E18 retinal conditioned medium

E18 retinal conditioned medium preparation was performed as previously described (Xia and Ahmad, 2016a). Briefly, E18 retinal cell dissociates were plated at a density of 1×10^5 cells/cm^2 in RCM with 2% KOS. After 3 days, the E18 conditioned medium was collected, centrifuged, filtered using 0.2 μm filters, and stored in −80 °C until use.

2.5. Retinal explant culture

The retinal explant cultures were performed as previously described (Xia and Ahmad, 2016a). E18 retinae were placed on a 0.4 μm semi-permeable membrane (Millipore, Temecula, CA), with the retina ganglion cell (RGC) layer side up, and cultured with RCM and 10% fetal bovine serum (FBS) for 10 days.

2.6. Quantitative polymerase chain reaction

mRNA and miRNA were isolated from cell and explant samples using TriZol reagent (Life Technologies, Grand Island, NY) and the miRCURY RNA isolation kit (Exiqon, Woburn, MA). cDNA was synthesized from mRNA using SuperScript III reverse transcriptase kit (ThermoFisher, Waltham, MA) and cDNA from miRNA was synthesized using miScript II RT kit (Qiagen, Valencia, CA). Transcripts were amplified using gene-specific primer (Supplement Table 1) and SYBR green PCR kit (Qiagen, Valencia, CA) with the RotorGene 600 (Corbett Robotics, San Francisco, CA). All qPCR results measured each sample in triplicate and no-template blanks were used for negative controls. Amplification curves and gene expressions were normalized to the house keeping gene *GAPDH* (for mRNA) and *U6* snRNA (for miRNA), used as an internal standard.

2.7. Immunofluorescence analysis

Immunofluorescence analysis for specific proteins was carried out as previously described (Xia and Ahmad, 2016a). Cryostat tissue sections, coverslips, and chamber slides were fixed with 4% paraformaldehyde (PFA) and blocked in blocking solution [5% NDS or NGS, and TritonX-100 (0.4% or 0.2% for nuclear or cytoplasmic staining, respectively), diluted in 1× PBS] for 30 min at RT. Samples were incubated in primary antibody solutions (specifications shown in Supplement Table 2) overnight at 4 °C and in secondary antibodies (Cy3) for 2 h at RT. Samples were mounted using VectaShield (Vector Laboratories, Burlingame, CA) and images were taken using a Zeiss AX10 fluorescence microscope accompanied with AxioVision Rel. 4.8 software. For quantification of the percentage of specific cell types in each experiment, cell type-specific antigen-positive cells were counted in 15 randomly selected fields in three wells (5 fields each) of 8-well-chamber slides or 3 cover slips (5 fields each). Quantification of cells was carried out as the percentage of GFP^+ cells expressing immunoreactivities to cell type-specific markers.

2.8. Fluorescent activated cell sorting (FACS) analysis

FACS analysis was carried out as previously described (Xia and Ahmad, 2016a). Differentiated neurospheres cells were dissociated and blocked for 30 min in 1× PBS containing 5% NGS and 0.3% Saponin. Cells were incubated in primary antibody for 1 h at RT followed by 1 h at 4 °C and in secondary antibody for 1 h at RT. IgG was used for setting the gate of fluorescent activated cell sorting (FACS). For sorting of GFP^+ cells, transduced E18 cells were suspended in cell sorting buffer (1× HBSS Phenol Red-, 2% FBS, 25 mM HEPES, 1 mM EDTA). The GFP^+ and GFP^- cells were sorted based on the defined gate, using E18 retinal cells transduced with lentiviruses without GFP.

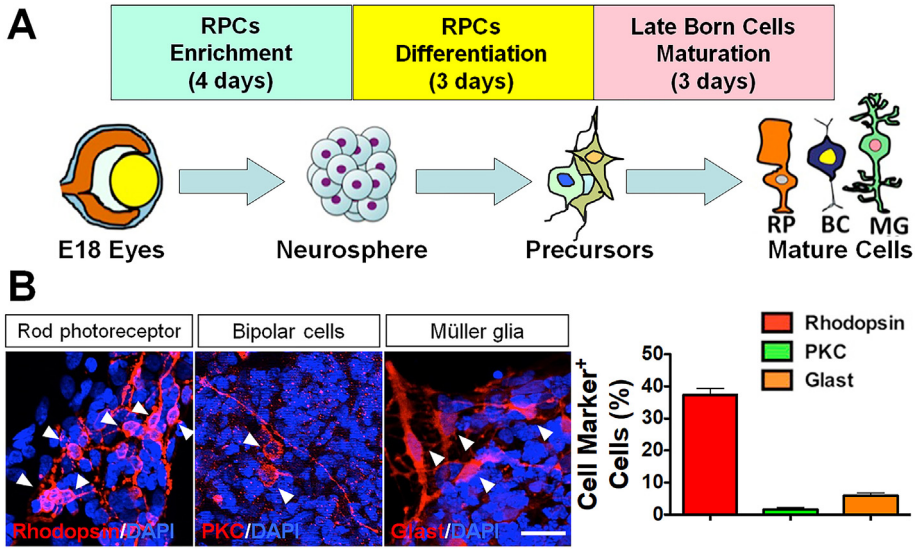

Fig. 1. The *in vitro* model simulates late retinal histogenesis. (**A**) A schematic representation of the *in vitro* model of late retinal histogenesis. (**B**) The generation of late born cells was confirmed by the expression of immunoreactivities corresponding to RPs (Rhodopsin), BCs (PKC), and MG (Glast). The proportion of late born cells is plotted in the right hand graph. Scale bar, 20 μm (B).

2.9. GO analysis of predicted targets of miR-29

The *miR-29* predicted target mRNAs were obtained from TargetScan (www.targetscan.org). The enrichment of gene ontology (GO) term in *miR-29* predicted target mRNAs were analyzed using DAVID online tools (Huang et al., 2007) (david.abcc.ncifcrf.gov) and Gene Ontology Consortium (geneontology.org). GO terms corresponding to biological process (BP_FAT) were selected. The enrichment of GO terms was determined by the *P*-value from DAVID online tool analysis. The *P*-values were determined by a modified Fisher's exact test, adjusted by the Benjamini-Hochberg method. The list of *miR-29c* predicted mRNA targets in specific GO term was obtained from Gene Ontology Consortium.

2.10. Statistical analysis

Values were expressed as mean ± SEM. Data were analyzed using unpaired two-tail *t*-test or one-way analysis of variance (ANOVA) for pairwise or multiple group comparisons, respectively (GraphPad Prism Software). *P* values < 0.05 were considered significant.

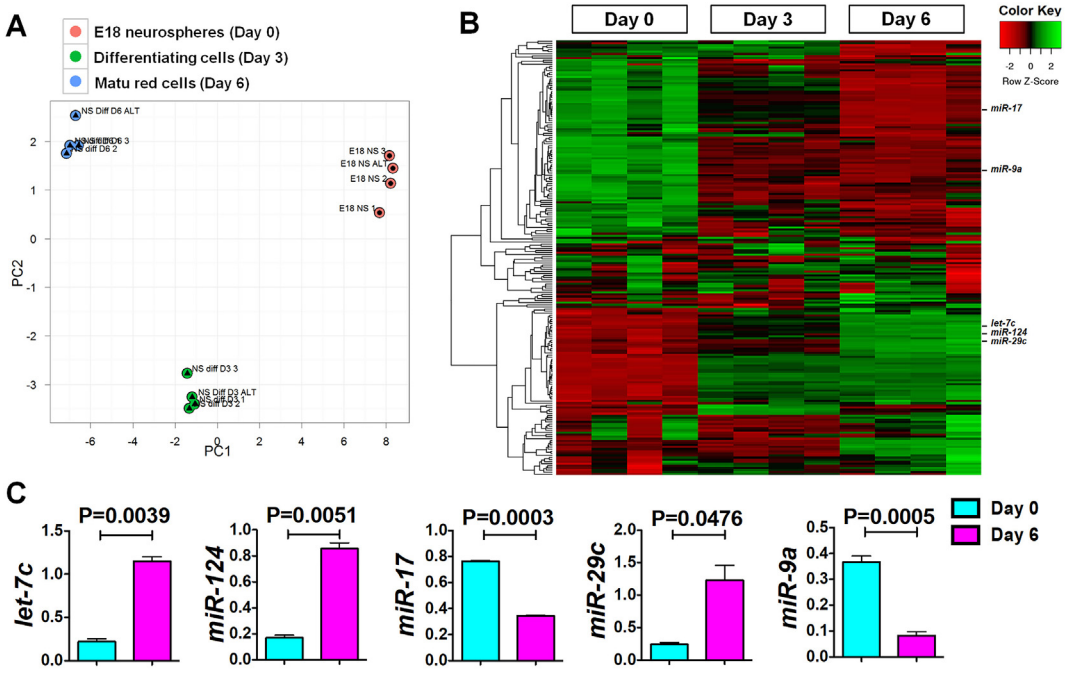

Fig. 2. Differentially expressed miRNAs during RPCs differentiation. (**A**) PCA plot of differentially expressed miRNAs in the three stages of RPCs differentiation. Each dot represents a single sample for each stage. The principal component analysis was performed on all samples, and on the top 50 microRNAs with the highest standard deviation. The normalized log ratio values have been used for the analysis. (**B**) The stage-specific differentially expressed miRNAs are represented in the heat map and hierarchical clustering-based dendrograms. (**C**) The microarray data was validated by examining the expression patterns of randomly selected miRNAs using qPCR. Amplification curves and the gene expressions were normalized to *U6* snRNA. Data are mean ± s.e.m.

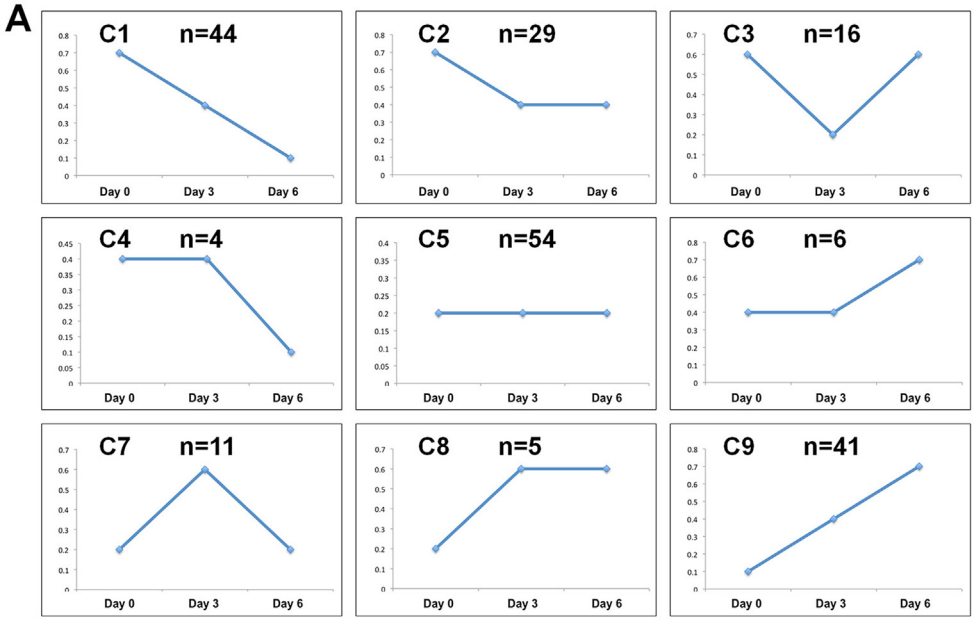

B

C1 n=44	let-7i-5p, miR-106b-3p, miR-106b-5p, miR-130a-3p, miR-130b-3p, miR-130b-5p, miR-148b-3p, miR-15b-5p, miR-16-5p, miR-17-1-3p, miR-17-5p, miR-1949, miR-19a-3p, miR-19b-3p, miR-204-5p, miR-207, miR-20a-5p, miR-20b-5p, miR-25-3p, miR-296-3p, miR-298-5p, miR-299a-5p, miR-301a-3p, miR-30b-3p, miR-32-5p, miR-320-3p, miR-324-3p, miR-325-3p, miR-325-5p, miR-34a-5p, miR-34b-3p, miR-34b-5p, miR-361-5p, miR-423-3p, miR-551b-3p, miR-652-3p, miR-674-5p, miR-7a-5p, miR-92a-3p, miR-92b-3p, miR-93-5p, miR-9a-3p, miR-9a-5p, miR-9b-5p
C2 n=29	let-7d-3p, miR-134-3p, miR-138-2-3p, miR-181a-2-3p, miR-195-5p, miR-331-5p, miR-340-5p, miR-342-3p, miR-347, miR-34c-3p, miR-34c-5p, miR-3568, miR-3571, miR-3572, miR-363-5p, miR-382-3p, miR-448-5p, miR-450a-3p, miR-466b-2-3p, miR-466b-5p, miR-466c-3p, miR-466c-5p, miR-493-5p, miR-668, miR-672-5p, miR-708-5p, miR-743b-3p, miR-7a-2-3p, miR-883-5p
C3 n=16	miR-129-5p, miR-135a-5p, miR-136-5p, miR-150-5p, miR-210-3p, miR-26b-5p, miR-29b-3p, miR-30e-5p, miR-32-3p, miR-328b-3p, miR-33-5p, miR-331-3p, miR-335, miR-344b-1-3p, miR-344b-2-3p, miR-384-3p
C4 n=4	miR-124-5p, miR-465-5p, miR-664-3p, miR-99b-3p
C5 n=54	let-7a-5p, let-7d-5p, let-7e-5p, miR-103-3p, miR-1249, miR-125a-5p, miR-129-1-3p, miR-129-2-3p, miR-1306-5p, miR-140-3p, miR-140-5p, miR-142-3p, miR-151-5p, miR-181c-5p, miR-1843-5p, miR-186-5p, miR-190a-5p, miR-190b-5p, miR-205, miR-26a-5p, miR-26b-3p, miR-292-3p, miR-2985, miR-3072, miR-30a-5p, miR-30b-5p, miR-30c-5p, miR-30d-5p, miR-30e-3p, miR-328a-3p, miR-329-3p, miR-329-5p, miR-338-3p, miR-352, miR-3541, miR-3577, miR-3586-5p, miR-362-3p, miR-376b-5p, miR-382-5p, miR-466b-1-3p, miR-466d, miR-483-3p, miR-484, miR-487b-5p, miR-487b-3p, miR-499-5p, miR-543-5p, miR-664-1-5p, miR-742-3p, miR-7b, miR-872-5p, miR-98-5p, miR-99b-5p
C6 n=6	miR-127-3p, miR-191a-5p, miR-21-5p, miR-214-3p, miR-23b-3p, miR-872-3p
C7 n=11	let-7a-2-3p, miR-183-3p, miR-1839-3p, miR-1843-3p, miR-185-3p, miR-3068-5p, miR-30c-1-3p, miR-320-5p, miR-431, miR-433-5p, miR-500-3p
C8 n=5	miR-194-3p, miR-3573-3p, miR-485-3p, miR-505-5p, miR-667-3p
C9 n=41	let-7b-5p, let-7c-5p, let-7f-5p, miR-101a-3p, miR-101b-3p, miR-107-3p, miR-124-3p, miR-125b-5p, miR-138-5p, miR-181a-1-3p, miR-181a-5p, miR-181b-5p, miR-181d-5p, miR-182, miR-183-5p, miR-185-5p, miR-204-3p, miR-21-3p, miR-218a-5p, miR-22-3p, miR-24-3p, miR-27b-3p, miR-294, miR-29c-3p, miR-300-5p, miR-341, miR-351-5p, miR-3584-3p, miR-3594-3p, miR-3596c, miR-378a-3p, miR-423-5p, miR-503-5p, miR-542-5p, miR-598-3p, miR-664-2-5p, miR-665, miR-675-5p, miR-758-5p, miR-877, miR-96-5p

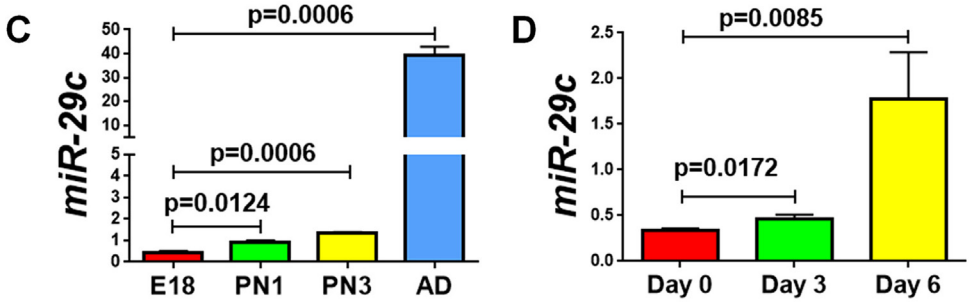

Fig. 3. The SOM algorithm identified clusters of miRNAs expressed during RPCs differentiation. (**A**) miRNAs expression profiles during RPCs differentiation were classified into 9 clusters by the SOM algorithm. Y-axis indicates relative expression levels of miRNAs and X-axis indicates the time points of RPCs differentiation. n, number of miRNAs in the cluster. (**B**) Member miRNAs in the Identified SOM clusters. (**C**) The expression levels of *miR-29c* increased with time during late retinal histogenesis and RPCs differentiation *in vitro*. Amplification curves and the gene expressions were normalized to *U6* snRNA. Data are mean ± s.e.m. Experiments were carried out three times in triplicates with 10–12 E18 embryos per group for *in vitro* perturbation.

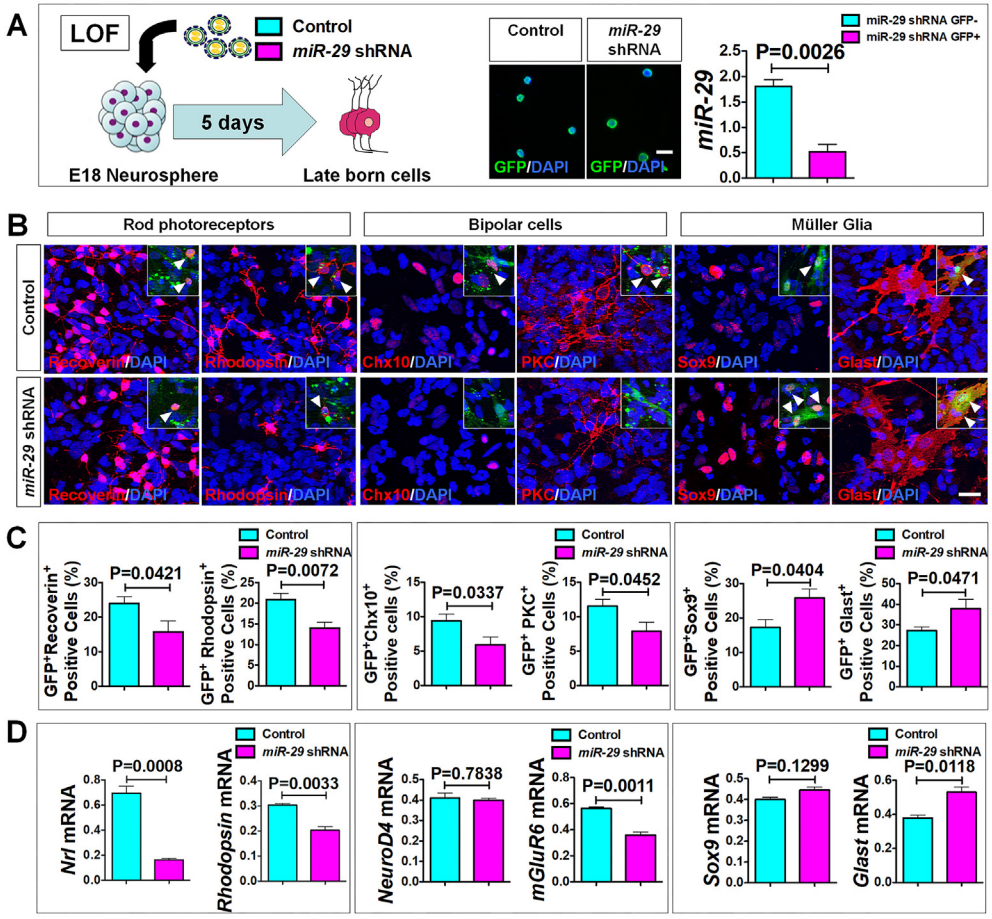

Fig. 4. *miR-29c* LOF inhibits neurogenesis and promotes gliogenesis *in vitro*. (**A**) A schematic representation of the experimental approach; E18 neurospheres were transduced with *miR-29c* shRNA+GFP/control GFP lentiviruses and subjected to differentiation for 5 days (left panel). The transduction efficiency was examined by the direct observation of GFP epifluorescence. qPCR analyses of GFP+ and GFP- cells sorted by FACS after transduction (middle panel), revealed a significant decrease in the expression of *miR-29c*, compared to controls, validating the *miR-29c* LOF approach (right panel). (**B**) Lentivirus transduced cells (GFP^+ cells) co-expressed RP (Recoverin/Rhodopsin)-, BC (Chx10/PKC)-, and MG (Sox9/Glast)-specific immunoreactivities (arrowheads) in the *miR-29c* LOF and control groups. (**C**) Quantification of GFP^+ cells co-expressing cell type-specific immunreactivities demonstrated a significant decrease in the proportions of RPs & BCs, and increase in that of MG in the *miR-29c* LOF group than in controls. (**D**) qPCR analysis of differentiated cells revealed a significant decrease and increase in levels of transcripts corresponding to regulators and markers of RPs (*Nrl*/*Rhodopsin*) & BCs (*Chx10*), and MG (*Glast*), respectively, in the *miR-29c* LOF group versus controls. No change in the levels of *NeuroD4* and *Sox9* transcripts were observed. Amplification curves and the gene expressions were normalized to *U6* snRNA (for miRNAs) and the housekeeping gene *GAPDH* (for genes). Scale bar, 20 μm (B, D). Data are mean ± s.e.m. Experiments were carried out three times in triplicates with 10–12 E18 embryos per group for *in vitro* perturbation.

3. Results

3.1. Temporal expression of miRNAs during differentiation of late RPCs

During late retinal histogenesis, RPCs differentiate into three different cell types: RPs, BCs, and MG. To examine the involvement of miRNAs in late histogenesis we have established an *in vitro* model where enriched late RPCs are differentiated into late born neurons and glia under controlled conditions (Parameswaran et al., 2014; Xia and Ahmad, 2016a; Xia et al., 2018) (Fig. 1A). Quantification of differentiated cells expressing cell type-specific markers revealed that in this model system RP, BC, and MG are generated in a similar proportion as *in vivo* where neurons (RP and BC), are predominant cells born, compared to glia (MG) (Fig. 1B). To identify miRNAs that might influence the differentiation of neurons and glia, we carried out miRNA microarray analysis on late RPCs in different stages of differentiation. These stages included day 0 (D0; undifferentiated stage), D3 (intermediate differentiation), and D6 (differentiated stage). Analysis of data revealed that of the 694 miRNAs annotated in miRBase 18.0, 213 miRNAs were expressed in retinal cells in the three stages examined. Next, we carried out principal component analysis (PCA), which demonstrated significant biological variations, based on differentially expressed miRNAs, between cells at different stages (Fig. 2A). Heat maps and hierarchical clustering-based dendrograms of cells in different stages of differentiation showed stage-specific differential expression of 213 miRNAs, in which their expression patterns at day 3 had changed, compared to those at day 0, suggesting their involvement in the differentiation of RPCs (Fig. 2B). Of all the differentially expressed miRNAs (154 out of 213; $p < 0.05$) between day 0 and day 6, 46 were up regulated and 52 were downregulated by at least 2 folds (Supplemental Table 3). A subset of miRNAs whose expression differed by 4 folds between day 0 and day 6 (upregulated: 29 miRNAs; downregulated: 22 miRNAs) were randomly selected for qPCR analysis to corroborate miRNA microarray results (Fig. 2C). Next, to identify miRNAs involved in differentiation through their dynamic expression profile we used the Self Organization Map (SOM) algorithm to analyze our microarray data. Nine clusters were created to represent the dynamic expression patterns in the data set at three different stages of differentiation (Fig. 3A and B). For example, clusters 1, 2, and 4 showed a trend of decrease in miRNA expression with time. In contrast, clusters 6, 8, and 9 showed a general trend of temporal increase in the expression of specific miRNAs. Clusters 3 and 7 included miRNAs with inverse expression patterns between the two developmental stages, whereas cluster 5 contained miRNAs with no significant changes in the expression during late histogenesis. We further examined miRNAs in cluster 9, whose expression patterns, as opposed to those in cluster 1, suggested their positive involvement in RPC differentiation, as exemplified by *let-7* (Hackler et al., 2010; Xia et al., 2016a). In this cluster we identified *mir-29c* for examining the functional involvement of a specific miRNA in neurogliogenesis. Further evidence that *mir-29c* might be involved in late histogenesis was its similar temporal expression patterns during late histogenesis *in vivo* and RPCs differentiation *in vitro* (Fig. 3C and D).

3.2. miR-29c is involved in neurogliogenic decision of RPCs

In order to examine the involvement of *miR-29* in late RPCs differentiation, we carried out the perturbation of function approach in the *in vitro* model of late histogenesis described above. Both *miR-29* loss-of-function (LOF) and gain-of-function (GOF) approaches were used. In

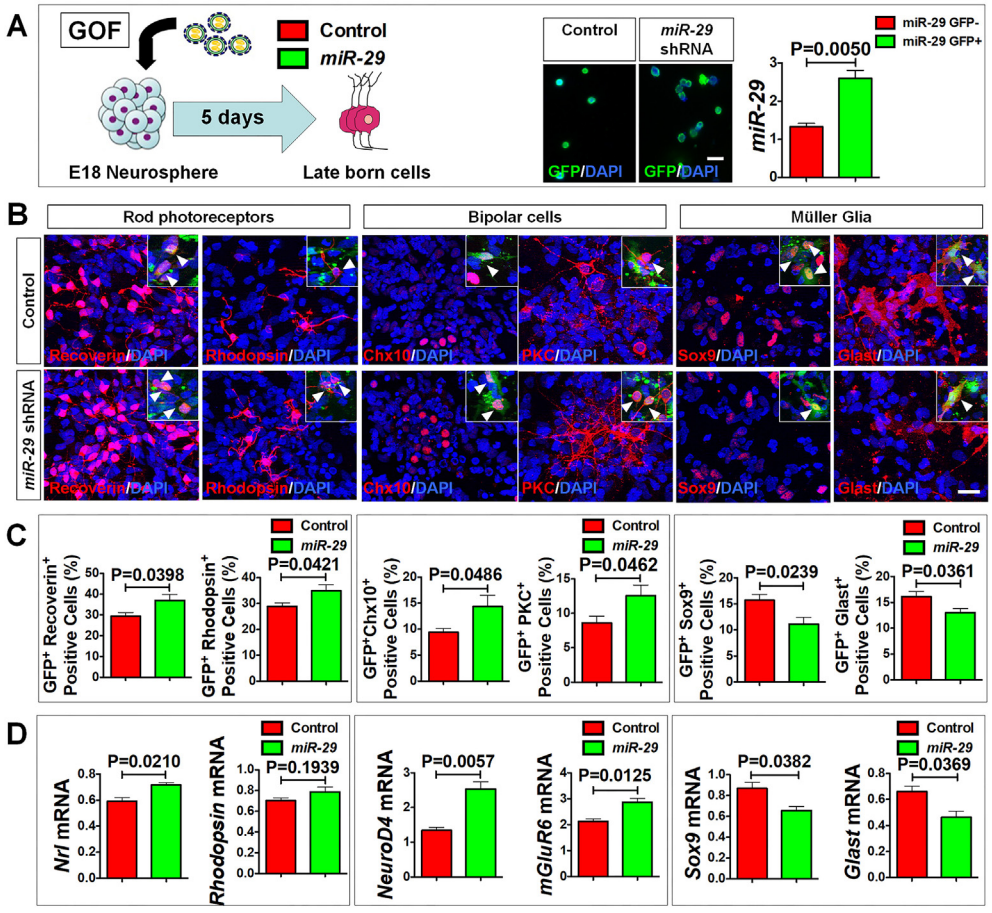

Figure 5. *miR-29c* GOF promotes neurogenesis and inhibits gliogenesis *in vitro*. (**A**) A schematic representation of the experimental approach; E18 neurospheres were transduced with *miR-29c*+GFP/control GFP lentiviruses and subjected to differentiation for 5 days (left panel). The transduction efficiency was examined by the direct observation of GFP epifluorescence (middle panel). qPCR analyses of GFP+ and GFP- cells sorted by FACS after transduction, revealed a significant increase in the expression of *miR-29c*, compared to controls, validating the *miR-29c* GOF approach (right panel). (**B**) Lentivirus transduced cells (GFP^+ cells) co-expressed RP (Recoverin/Rhodopsin)-, BC (Chx10/PKC)-, and MG (Sox9/Glast)-specific immunoreactivities (arrowheads) in the *miR-29c* and control groups. (**C**) Quantification of GFP^+ cells co-expressing cell type-specific immunreactivities demonstrate a significant increase in the proportions of RPs & BCs, and decrease in that of MG in the *miR-29c* group than in controls. (**D**) qPCR analysis of differentiated cells revealed a significant increase and decrease in levels of transcripts corresponding to regulators and markers of RPs (*Nrl/Rhodopsin*) & BCs (*NeuroD4/Chx10*), and MG (*Sox9/Glast*), respectively, in the *miR-29c* group versus controls. Amplification curves and the gene expressions were normalized to *U6* snRNA (for miRNAs) and the housekeeping gene *GAPDH* (for genes). Scale bar, 20 μm (B, D). Data are mean ± s.e.m. Experiments were carried out three times in triplicates with 10–12 E18 embryos per group for *in vitro* perturbation.

the LOF approach neurosphere-enriched late RPCs were transduced with a dual-promoter lentivirus that expressed either *miR-29c* shRNA+GFP (=LOF group) or *miR-29c* scrambled shRNA+GFP (=control group) and cultured in differentiation conditions for 5 days *in vitro* (DIV) (Fig. 4A; left panel). The efficiency of transduction, as measured by GFP^+ cells, was ~80% (Fig. 4A; middle panel). Quantitative PCR (qPCR) analyses of FACS sorted GFP^+ cells revealed ~75% decrease in *miR-29c* levels in the LOF groups, compared to controls (Fig. 4A; left panel), indicating the specificity of the LOF approach (Fig. 4A). *miR-29c* shRNA also inhibited levels of *miR-29a* and *miR-29b* as expected, given the extensive homology among *miR-29* family members (Supplement Fig. 1). We observed a significant decrease in the proportion of GFP^+ cells expressing immunoreactivities characteristic of RPs (recovering and rhodopsin) and BCs (Chx10 and PKC), compared to controls, suggesting the association of *miR-29c* LOF with decreased neuronal differentiation (Fig. 4B and C). In contrast, the proportion of GFP^+ cells expressing immunoreactivities characteristic of MG (Sox9 & Glast) significantly increased compared to controls, suggesting that *miR-29c* LOF was associated with increased gliogenesis (Fig. 4B and C). The decrease in the levels of transcripts corresponding to RPs (*Nrl, rhodopsin*) and BCs (*mGluR6*) and increase in those of MG (*Glast*) corroborated the results, ascertained by examining the cell-type specific protein markers (Fig. 4D). However, the levels of *NeuroD4* (BC) and Sox9 (MG) mRNAs remain unchanged, presumably due to their persistent expression in progenitor/precursor populations. Next, to examine whether or not the ectopic expression of *miR-29c* promoted neuronal differentiation at the expense of gliogenesis, as suggested by *miR-29c* LOF, we carried out *miR-29c* GOF experiments during RPC differentiation. The approach involved transduction of neurosphere-enriched late RPCs with a dual-promoter lentivirus that expressed *miR-29c* + GFP (=GOF groups) or scrambled sequence + GFP (=control groups) (Fig. 5A, left panel). The transduction efficiency and specificity was determined as above, where the misexpression was reflected in significant increase in the levels of *miR-29c*, versus controls (Fig. 5A, middle and right panel). In contrast to results obtained by *miR-29c* LOF, the proportions of RP and BC increased, as judged by the expression cell-type specific markers (Fig. 5B and C) and transcripts (Fig. 5D), and that of MG decreased compared to controls, confirming that *miR-29c* expression was preferentially associated with neuronal differentiation. All cell-type specific transcripts, with the exception of *rhodopsin*, showed significant changes in their levels in response to *miR-29c* GOF, corroborating results obtained by immunocytochemical analysis. Next, to address the concern that these results might be a function of *in vitro* condition where cell-cell interactions necessary for the differentiation was compromised, we carried out *miR-29c* perturbation experiments in retinal explants *ex-vivo*. Both the *miR-29c* LOF (Supplement Fig. 2) and GOF (Supplement Fig. 3) approaches confirmed the results obtained using the neurosphere culture; the former suppressed neuronal differentiation and promoted gliogenesis while the latter facilitated neuronal differentiation at the expense of gliogenesis, as ascertained by levels of cell-type specific protein markers and transcripts. Taken together, these results suggested that *miR-29c* promotes neuronal differentiation during late histogenesis.

3.3. *miR-29c regulates neurogliogenic decision of RPCs through REST*

To understand the underlying mechanism of *miR-29c* influence on the retinal neurogliogenesis, we first examined the predicted targets of *miR-29* using the miRNA target prediction database, Targetscan. Gene ontology (GO) analysis using GO Slim Classification of 818 putative *miR-2c* target genes identified "biological regulation" and "developmental process" as among the top 5 functional clusters (Fig. 6A). Analysis of the

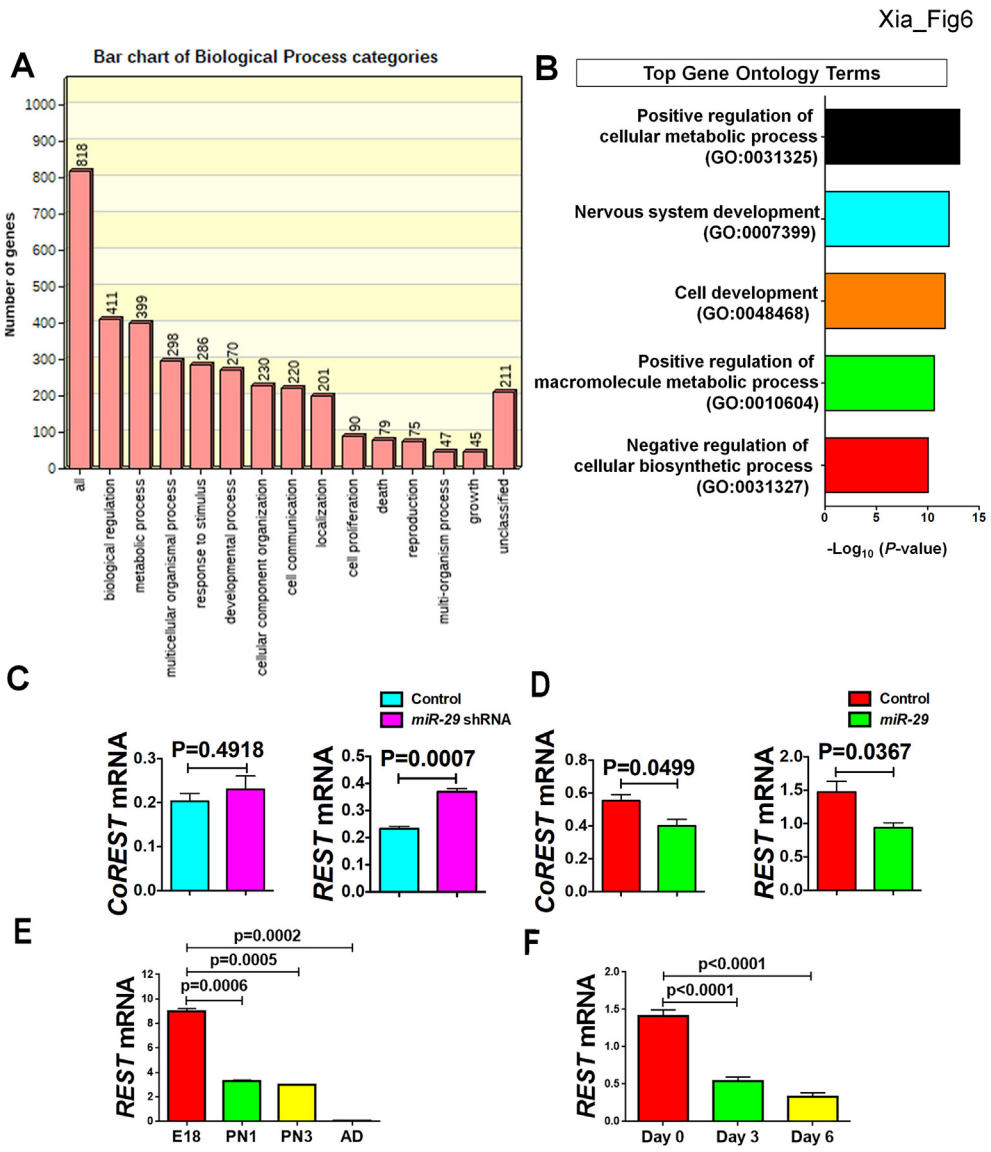

Fig. 6. REST is a putative target of *miR-29c*. (**A**) The GO Slim summary of GO analysis of *miR-29c* predicted target genes identified "biological function" and "developmental process" terms as top biological processes. (**B**) GO analysis of *miR-29c* predicted target genes identified "Nervous system development" as one of the most enriched GO term. (**C**) The expression of *REST*, the candidate *miR-29c* target gene identified GO term, was determined by qPCR in both *miR-29c* LOF and GOF conditions. (**D**) The expression levels of *REST* decreased with time during late retinal histogenesis *in vivo* and RPCs differentiation *in vitro*. Amplification curves and the gene expressions were normalized to the housekeeping gene *GAPDH*. Data are mean ± s.e.m. Experiments were carried out three times in triplicates with 10–12 E18 embryos per group for *in vitro* perturbation.

targets in the "biological regulation" class using the DAVID bioinformatics platform and Panther Classification System demonstrated Nervous System Development (GO: 0007399) as one of the most enriched GO terms (Fig. 6B). Further filtering Regulation of Nervous System Development (GO: 0051960) for putative *miR-29c* targets revealed 95 genes (Supplemental Table 4). Next, we carried out literature search of genes involved in the regulation of stem cells to select 6 genes out of the 95 candidate genes. Out of the 6 genes (*PTEN, LIF, Co-REST, CCND1, Hey2, and REST*) we selected REST because (1) it is a negative regulator of neuronal differentiation (Ballas et al., 2005), (2) REST has been identified as a direct target of repression by miR 29c (Duan et al., 2014) and (3) REST expression in RPCs showed negative correlation with that of miR 29c (see below). Therefore, we examined the expression of *REST* under *miR-29c* LOF and GOF conditions in late RPCs. We observed that transcripts corresponding to *REST* increased and decreased significantly, compared to controls in *miR-29c* LOF and GOF conditions, respectively, suggesting that *REST* may be a valid target of *miR-29c* to promote RPC differentiation, preferentially along the neuronal lineage (Fig. 6C). We tested the premise as follows: First, we determined the temporal expression patterns of REST during late retinal histogenesis *in vivo* and compared them with those during the differentiation of RPCs *in vitro*. We observed a decrease in *REST* transcript levels with time, with largest drop between E18 and PN1, when neuronal differentiation is at its peak (Fig. 6D). *REST* transcript levels further declined in the adult retina. Similarly, a temporal decline in REST transcript levels was observed as RPCs differentiated through the three stages of differentiation *in vitro* (Fig. 6E). This temporal decline of *REST* expression was inverse of *miR-29c* expression both *in vivo* (Fig. 3C) and *in vitro* (Fig. 3D), further suggesting that *REST* is targeted by *miR-29c* during the differentiation of the late retinal RPCs. Second, we tested the premise that the negative influence of *miR-29c* shRNA on neuronal differentiation of RPCs could be abrogated by independent silencing of *REST* expression (Fig. 7). The late RPCs were divided into three groups: control group (transduced with *miR-29c* scrambled shRNA+GFP and scrambled siRNA+GFP lentivirus), *miR*-29 shRNA group (transduced with *miR-29c* shRNA+GFP lentivirus), and *miR*-29 shRNA + REST siRNA group (transduced with *miR-29c* shRNA+GFP & REST siRNA+GFP lentivirus) (Fig. 7A; left panel). The qPCR results revealed that the *REST* expression, which increased in response to *miR-29c LOF,* was significantly repressed by siRNA-mediated silencing of REST (Fig. 7A; Right panel). Quantification of cell type-specific markers and transcripts as above revealed that the silencing of REST significantly restored the proportions of RPs and BCs that were reduced in response to *miR-29c LOF* (Fig. 7B, C, D). In contrast, silencing of REST significantly reduced the proportion of MG that had increased in

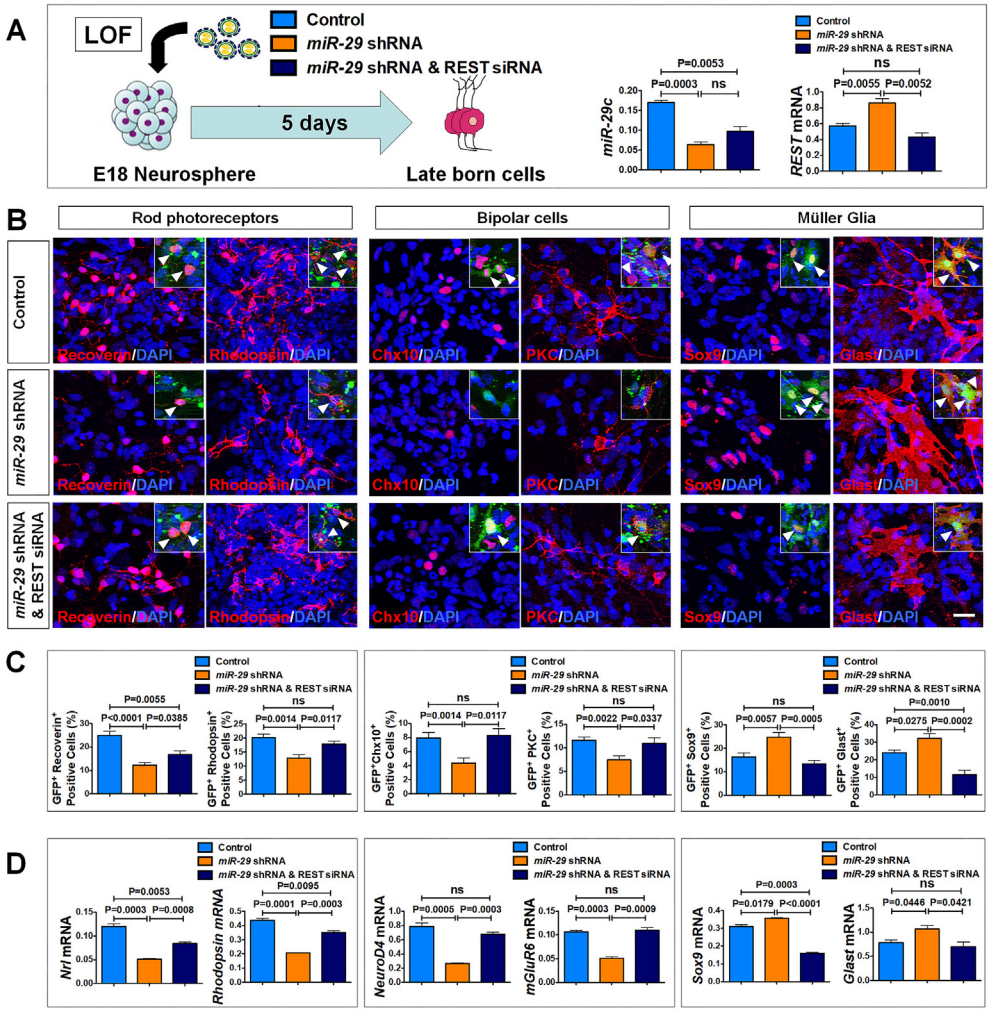

Fig. 7. *miR-29c* influence on neurogliogenesis is mediated through REST. (**A**) A schematic representation of the experimental approach; E18 neurospheres were transduced with *miR-29c* shRNA+GFP/control GFP lentiviruses and subjected to differentiation for 5 days (left panel). A subgroup in *miR-29c* LOF was co-transfected with REST siRNA to inhibit REST expression. qPCR analysis demonstrated similar decrease in *miR-29c* levels in the *miR-29c* LOF subgroups, with or without REST siRNA co-transfection, compared to controls (middle panel). The up-regulation of REST in *miR-29c* LOF was eliminated by REST siRNA treatment (left panel). (**B**) Lentivirus transduced cells (GFP^+ cells) co-expressed RP (Recoverin/Rhodopsin)-, BC (Chx10/PKC)-, and MG (Sox9/Glast)-specific immunoreactivities (arrowheads) in three experimental groups. (**C**) The proportions of GFP^+ & $Recover^+$/$Rhodopsin^+$/$Chx10^+$/PKC^+ cells and GFP^+ & $Sox9^+$/$Glast^+$ cells, which decreased and increase in the *miR-29c* LOF group, respectively, were restored by REST siRNA treatment (**D**) qPCR analysis revealed a decrease and increase in the transcripts corresponding to RPs (*Nrl/Rhodopsin*) & BC (*NeuroD4/mGluR6*)- and MG (*Sox9/Glast*)-specific genes in the *miR-29c* LOF group, compared to controls. The effects of *miR-29c* LOF were abrogated in the presence of REST siRNA. Amplification curves and the gene expressions were normalized to *U6* snRNA (for miRNAs) the housekeeping gene *GAPDH* (for genes). Scale bar, 20 μm (D). Data are mean ± s.e.m. Experiments were carried out three times in triplicates with 10–12 E18 embryos per group for *in vitro* perturbation.

response to *miR-29c LOF*. Furthermore, similar results were obtained when these double transduction experiments were carried out *ex-vivo* in retinal explants (Supplemental Fig. 4). Taken together, these results suggested that *REST* transcripts were targeted by *miR-29c*-mediated repression for facilitating neuronal differentiation during late histogenesis. Lastly, given the recent evidence that REST may affect development by influencing cell cycle regulation (Zhang et al., 2017a), we examined whether or not *miR-29c*-mediated differentiation involved facilitation of cell cycle exit. We misexpressed *miR-29c* in late RPCs and cultured them in proliferation condition for 5 DIV followed by examination of the expression of cell cycle regulators. We observed a significant decrease in immunoreactivities corresponding to proliferation antigen, Ki67 in *miR-29c* GOF groups, compared to controls (Fig. 8A–C). That misexpression of *miR-29c* in late RPCs negatively influenced their proliferation was corroborated by decreased levels of transcripts corresponding to proliferative cell nuclear antigen (*PCNA*) along with that of Ki67 in *miR-29c* GOF groups, compared to controls (Fig. 8D and E). Next, to know the mechanism underlying *miR-29c*-mediated inhibition of cell proliferation we examined the expression of transcripts corresponding to cyclin-dependent kinase inhibitors (CKIs), $p27^{Kip1}$ (*CDKN1B*) and $p21^{Cip1}$ (*CDKN1A*). CKIs directly inhibit the activity of cyclin-dependent kinase (cdk) complexes that control G1/S progression, thus causing G1 arrest (Sherr and Roberts, 1995). In contrast to levels of *PCNA* and *Ki67* transcripts, that of *p27kip1* increased in *miR-29c* GOF groups, compared to controls (Fig. 8F). When $p27^{Kip1}$ transcripts levels were examined in RPCs in which REST had been silenced by siRNA (Fig. 7), we observed that its levels were increased, compared to controls suggesting that the recruitment of $p27^{Kip1}$ for inhibiting cell cycle involved *miR-29c-REST* axis (Fig. 8 H). No significant differences were seen in $p21^{Cip1}$ transcripts levels, demonstrating the tissue specificity of $p27^{Kip1}$ in regulating developmental processes (Fig. 8 G, I). That the *miR-29c*-mediated cell cycle exit and differentiation may occur in a concert was suggested by the expression of regulators of neurons (*Nrl* and *NeuroD4*) and glia (*Sox9*) that increased and decrease, respectively, in *miR-29c* GOF groups versus controls in proliferation conditions (Fig. 8 J-L). Taken together, these observations suggested that *miR-29c* repressed *REST* for facilitating neuronal differentiation of late RPCs.

4. Discussion

The development of vertebrate retina entails progression of RPCs through distinct evolutionarily conserved stages for generating different cell types. Critical among them is the stage of late histogenesis when RPCs transition from generating neurons to glia. The mechanism underlying neurogliogenic decision, necessary for addressing the knowledge gap in retinal development (Centanin and Wittbrodt, 2014) and formulating approaches to unlock the dormant neurogenic potential of MG for therapeutic regeneration (Ahmad et al., 2011; Devoldere et al., 2019; Goldman, 2014; Xia and Ahmad, 2016b), remains poorly understood. Here, we have demonstrated that *miR-29c*, one of the 13 evolutionarily conserved miRNAs in our screen whose expression is associated with late histogenesis in mouse retina (Hackler et al., 2010), facilitates differentiation, favoring that of RPs and BCs over MG. This notion is supported by the following observations: first, the temporal expression

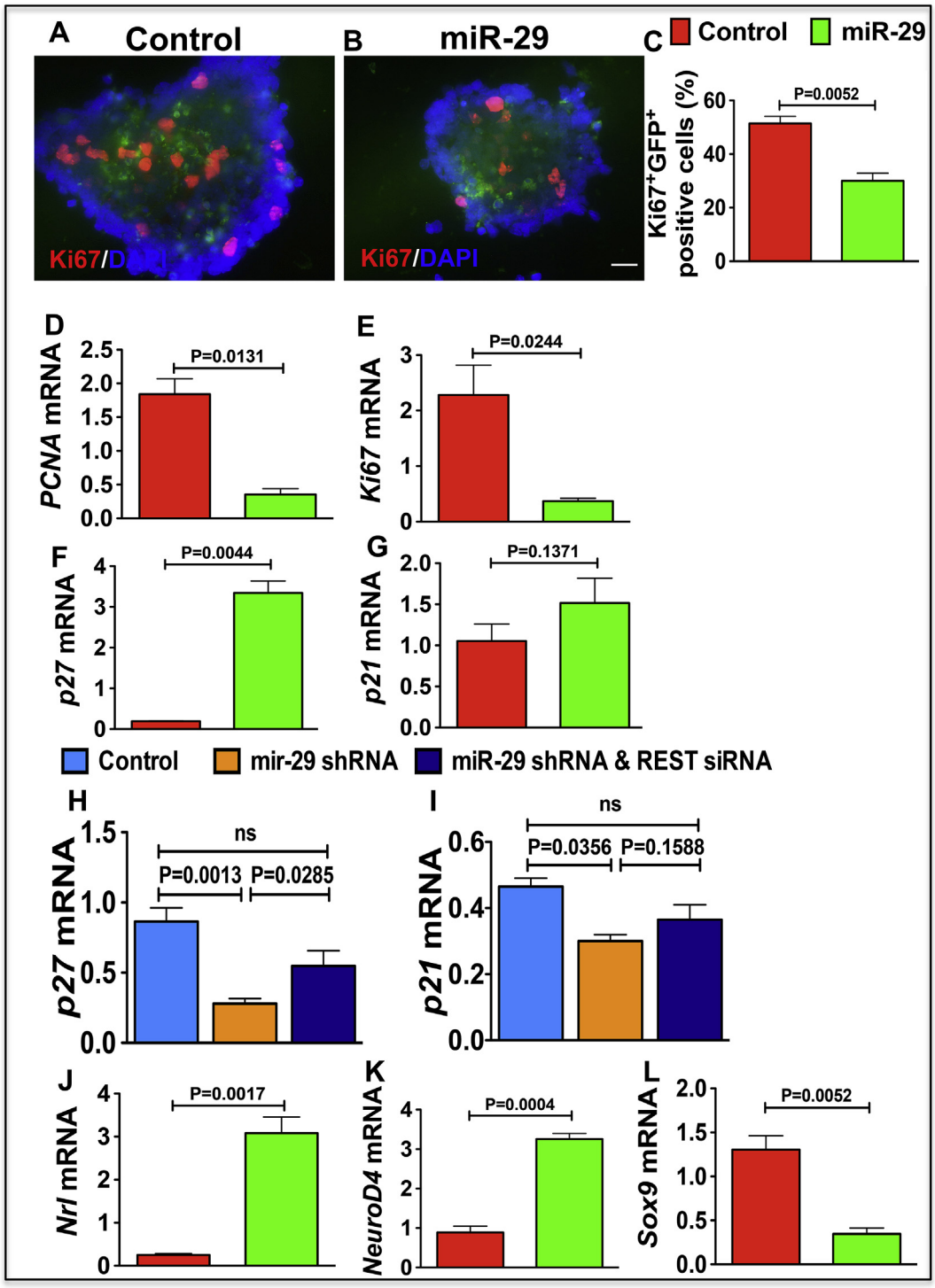

Fig. 8. *miR-29c* influences RPC proliferation. Late RPCs, transduced with *miR-29c*+GFP/control GFP lentiviruses, were cultured in proliferating condition for 5DIV and examined for indices of cell proliferation. (**A-C**) The proportions of Ki67^{+} cells were significantly less in *miR-29c* GOF neurospheres than in controls. (**D-E**) There was a significant decrease in *PCNA* and *Ki67* transcripts levels in *miR-29c* GOF neurospheres versus controls. (**F-G**) Levels of $p27^{kip1}$ transcripts increased and that of $p21^{Cip1}$ remained unchanged in *miR-29c* GOF neurospheres, compared to controls. (**H-I**) Levels of $p27^{kip1}$ transcripts increased and that of $p21^{Cip1}$ remained unchanged in the REST-siRNA treated group versus controls. (**J-L**) Levels of *Nrl* and *NeuroD4* transcripts increased and that of *Sox9* decreased in *miR-29c* GOF neurospheres versus controls. Scale bar, 20 μm (A). Data are mean ± s.e.m. Experiments were carried out three times in triplicates with 10–12 E18 embryos per group for *in vitro* perturbation.

patterns of *miR-29c* were similar during late histogenesis *in vivo* and in the *in vitro* model. Second, silencing of *miR-29c* in RPCs adversely affected their differentiation into RPs and BCs, with significant increase in the proportion of MG. In contrast, the ectopic expression of *miR-29c* facilitated RP and BC differentiation at the expense of the generation of MG. Lastly, silencing the expression of REST, restored neuronal differentiation, which was compromised in favor of glia due to a decrease in the expression *miR-29c* (Fig. 9).

However, contrary to our observation here, a recent study reported that *miR-29a* promoted the differentiation of RPCs regardless of the

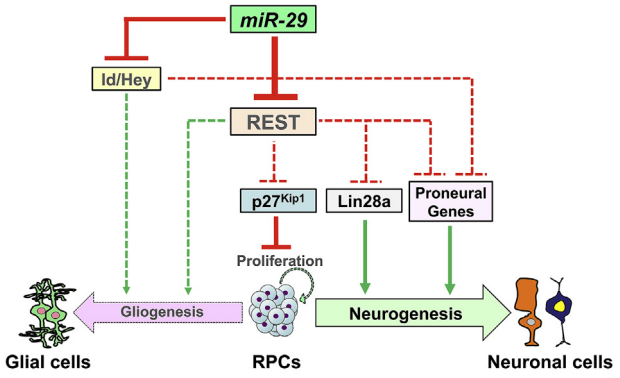

Fig. 9. Regulation of neurogliogenesis in RPCs by *miR-29* involvement. During late histogenesis *miR-29c* levels increases in RPCs, which negatively regulates the expression of *REST*. The *miR-29c*-mediated down regulation of REST may (1) facilitate neuronal differentiation by disinhibiting *Lin28* and/or proneural genes; (2) inhibit glial differentiation directly as neuronal-specific genes are removed from REST-mediated repression and indirectly by inhibiting gliogenic genes such as *Id* and *Hey*, and (3) inhibit RPC proliferation (broken curved arrow) by de-repressing p27Kip-mediated cell cycle exit.

neuronal or glial lineage (Zhang et al., 2017b). This difference is likely due to two reasons, which may not be mutually exclusive. First, the difference may be due to the functional diversity of *miR-29* family members. For example, *miR-29* family has two clusters (*miR-29a/b-1* and *miR-29b-2/c*) in two genomic loci (Garzon et al., 2009). These two clusters can be differentially regulated in normal and pathological conditions by various mechanisms during miRNA biogenesis (Garzon et al., 2009; Wu et al., 2010). The differential expression patterns of *miR-29* family members may result in different functional outcomes. For example, *miR-29a/b-1*, but not *miR-29b-2/c*, is involved in inducing trophoblast lineages in early differentiation of mouse embryonic stem cells (Cui et al., 2016). Second, though *miR-29a* and *miR-29c* may function differently in the regulation of late RPCs, we could not exclude the possibility that the different culture conditions and protocols used in (Zhang et al., 2017b) and our studies influenced the results. They used heterogeneous culture of PN1 retinal cells and promoted generic differentiation of RPCs by exposing them to FBS, which might have masked the influence of *miR-29a* on neuronal versus glial lineage. Besides, the use of GFAP, which is also expressed in RPCs, as the sole glial marker, might have further failed to reveal *miR-29a* effects on gliogenesis, if any (Zhang et al., 2017b). In contrast, we examined the effects of *miR-29c* in an *in vitro* model of late histogenesis, consisting of enriched E18 RPCs, where neurons (RP and BC) and glia (MG) were generated in proportions similar to those observed *in vivo*, ascertained by multiple markers for neurons and glia (Xia and Ahmad, 2016a; Xia et al., 2018).

Our observations regarding the involvement of *miR-29c* during differentiation complements other studies within (Shin et al., 2014; Zhang et al., 2017b) and without (Kapinas et al., 2009) the brain where the miRNA has been observed to promote differentiation of progenitors/precursors (Kapinas et al., 2009). However, our observations that *miR-29c* favors the differentiation of RPCs along one lineage over another suggests that it may be a part of a switch that helps regulate the binary cell fate of RPCs during late histogenesis. The switch may include the *miR-29c-REST* axis, which is defined by the inverse correlation between the developmental expression patterns of *miR-29c* and REST and their functional antagonism during the generation of RPs/BCs and MG. REST, which is a transcriptional repressor of neuronal genes (Ballas et al., 2005), and helps maintain the non-neuronal phenotype of glia (Abrajano et al., 2009) and non-neural cells (Duan et al., 2014), when repressed by *miR-29c* is likely to tip the balance during the differentiation of RPCs toward the neuronal lineage. Recently, it was demonstrated that *miR-29a* promoted neuronal differentiation of RPCs by silencing Rbm8A, one of the factors in the exon junction complex (Zhang et al., 2017b). Rbm8A is expressed in the sub-ventricular zone (SVZ) of the embryonic cortex; it maintains neuronal progenitors and loss of its expression is associated with neuronal differentiation (Zou et al., 2015). However, the mechanism underlying Rbm8A involvement in neuronal differentiation remains poorly understood, complicated further by the observation that Rbm8A appeared to negatively regulate REST (Zou et al., 2015), in which case a decrease in Rbm8A expression is likely to up-regulate REST expression, inhibiting neuronal differentiation.

Given the conserved nature of neurogliogenesis in the vertebrate retina, it is likely that *miR-29c-REST* axis interacts with other conserved regulators of neuronal differentiation to ensure the fidelity of the process. A parallel mechanism through which the *miR-29c*-mediated silencing of *REST* can help neurogliogenesis may involve the *Lin28* regulatory axis (Xia et al., 2018). For example, it has been recently observed that during retinal histogenesis the expression of *Lin28* was incompatible with MG differentiation and favored generation of neurons (Xia et al., 2018). It was demonstrated that *Lin28* effects on neurogliogenesis in the developing retina was mediated through the insulin like growth factor (Igf) signaling, which may enhance neurogenesis by activating MEK-ERK and PI3K-AKT-mTOR pathways (Bateman and McNeill, 2006). Given the observation that *Lin28* is a target of repression by REST (Johnson et al., 2008), *miR-29c*-mediated inhibition of REST may recruit *Lin28-Igf* axis to promote neuronal differentiation of the late RPCs. Additionally, our observations suggest that the influence of the *miR-29c-REST* axis on the differentiation of late RPCs may also include facilitating their exit from the cell cycle. This is likely achieved by the de-repression of $p27^{Kip1}$ gene when REST is inhibited by *miR-29c*. This notion is supported by (1) an increase in the expression of $p27^{Kip1}$ upon siRNA-mediated silencing of REST in late RPCs, (2) the presence of the *cis*-acting regulatory element for REST-mediated gene repression, RE-1 in $p27^{Kip1}$ gene (Bruce et al., 2004) and (3) the involvement of $p27^{kip1}$ in the regulation of RPCs during retinal development (Dyer and Cepko, 2001; Levine et al., 2000; Ogawa et al., 2017). It is also likely that *miR-29c* may also activate $p27^{Kip1}$ by influencing Notch signaling (see below). For example, it has been demonstrated that Notch signaling inhibits $p27^{Kip1}$ through Hes-mediated repression (Del Debbio et al., 2016). Therefore, repression of *Hes/Hey* transcripts by *miR-29c* would de-repress $p27^{kip1}$, thus facilitating cell cycle exit, which may occurr in concert with the activities of the *miR-29c-REST* axis to engage neural/neuronal genes by itself or through the *Lin28-Igf* axis.

While these observations shed light on differentiation in general, they do not explain how *miR-29c* expression becomes inhibitory to glial differentiation. This may also involve *REST*. For example, REST is known to influence gliogenesis by regulating the expression of multiple classes of genes involved in glial identity and function (Abrajano et al., 2009). Therefore, *miR-29c*-mediated repression of *REST* may destabilize glial differentiation program in RPCs. In parallel, *miR-29c* may also achieve this by inhibiting the BMP and Notch signaling pathways, two known regulators of MG differentiation, by repressing transcripts encoding their effectors, Id and Hes/Hey families of transcriptional repressors, respectively. For example, Id1, which negatively regulates proneural genes and is a target of *mir-29c* (Table 4), has been demonstrated to facilitate MG differentiation (Ueki et al., 2015). The Hes and Hey class of transcriptional repressors, of which *Hey1* and *Hey2* are *miR-29c* targets (Table 4), are known regulators of gliogenesis; their (Hes1/Hes5/Hey2) ectopic expression promotes the differentiation of MG (Furukawa et al., 2000). Therefore, *miR-29c*-mediated inhibition of Id and Hes/Hey families of repressors of proneural genes would destabilize gliogenesis in RPCs in favor of neuronal differentiation. Since Id1 is known to sustain Hes1 expression by suppressing Hes1 negative auto-regulation (Bai et al., 2007), its repression can independently inhibit Notch signaling-mediated gliogenesis. In summary, our results posit *miR-29c* as one of the regulators of neurogliogenesis in the retina by fine-tuning the expression of the key components of the regulatory axes such as REST. Since the targets of *miR-29c* are conserved regulatory genes in the retina, an integral part of

the CNS, it may play similar role during neurogliogenesis, elsewhere in the brain.

Conflicts of interest

None.

Acknowledgements:

Thanks are due to Helen Erickson for excellent technical help and editing of the manuscript. This work was supported by Pearson Foundation, National Eye Institute, Center of Biomedical Research Excellence (COBRE) grant, and Research to Prevent Blindness.

Appendix A. Supplementary data

Supplementary data to this article can be found online at https://doi.org/10.1016/j.ydbio.2019.03.013.

References

Abrajano, J.J., Qureshi, I.A., Gokhan, S., Zheng, D., Bergman, A., Mehler, M.F., 2009. Differential deployment of REST and CoREST promotes glial subtype specification and oligodendrocyte lineage maturation. PLoS One 4, e7665.

Ahmad, I., Del Debbio, C.B., Das, A.V., Parameswaran, S., 2011. Muller glia: a promising target for therapeutic regeneration. Invest. Ophthalmol. Vis. Sci. 52, 5758–5764.

Bai, G., Sheng, N., Xie, Z., Bian, W., Yokota, Y., Benezra, R., Kageyama, R., Guillemot, F., Jing, N., 2007. Id sustains Hes1 expression to inhibit precocious neurogenesis by releasing negative autoregulation of Hes1. Dev. Cell 13, 283–297.

Ballas, N., Grunseich, C., Lu, D.D., Speh, J.C., Mandel, G., 2005. REST and its corepressors mediate plasticity of neuronal gene chromatin throughout neurogenesis. Cell 121, 645–657.

Bateman, J.M., McNeill, H., 2006. Insulin/IGF signalling in neurogenesis. Cell. Mol. Life Sci. 63, 1701–1705.

Bruce, A.W., Donaldson, I.J., Wood, I.C., Yerbury, S.A., Sadowski, M.I., Chapman, M., Gottgens, B., Buckley, N.J., 2004. Genome-wide analysis of repressor element 1 silencing transcription factor/neuron-restrictive silencing factor (REST/NRSF) target genes. Proc. Natl. Acad. Sci. U. S. A. 101, 10458–10463.

Centanin, L., Wittbrodt, J., 2014. Retinal neurogenesis. Development 141, 241–244.

Cui, Y., Li, T., Yang, D., Li, S., Le, W., 2016. miR-29 regulates Tet1 expression and contributes to early differentiation of mouse ESCs. Oncotarget 7, 64932–64941.

Damiani, D., Alexander, J.J., O'Rourke, J.R., McManus, M., Jadhav, A.P., Cepko, C.L., Hauswirth, W.W., Harfe, B.D., Strettoi, E., 2008. Dicer inactivation leads to progressive functional and structural degeneration of the mouse retina. J. Neurosci. 28, 4878–4887.

Decembrini, S., Bressan, D., Vignali, R., Pitto, L., Mariotti, S., Rainaldi, G., Wang, X., Evangelista, M., Barsacchi, G., Cremisi, F., 2009. MicroRNAs couple cell fate and developmental timing in retina. Proc. Natl. Acad. Sci. U. S. A. 106, 21179–21184.

Del Debbio, C.B., Mir, Q., Parameswaran, S., Mathews, S., Xia, X., Zheng, L., Neville, A.J., Ahmad, I., 2016. Notch signaling activates stem cell properties of muller glia through transcriptional regulation and Skp2-mediated degradation of p27Kip1. PLoS One 11, e0152025.

Devoldere, J., Peynshaert, K., De Smedt, S.C., Remaut, K., 2019 Feb 4. Muller cells as a target for retinal therapy. Drug Discov. Today. https://doi.org/10.1016/j.drudis.2019.01.023 pii: S1359-6446(18)30431-8. [Epub ahead of print].

Duan, P., Sun, S., Li, B., Huang, C., Xu, Y., Han, X., Xing, Y., Yan, W., 2014. miR-29a modulates neuronal differentiation through targeting REST in mesenchymal stem cells. PLoS One 9, e97684.

Dyer, M.A., Cepko, C.L., 2001. p27Kip1 and p57Kip2 regulate proliferation in distinct retinal progenitor cell populations. J. Neurosci. 21, 4259–4271.

Ebert, M.S., Sharp, P.A., 2012. Roles for microRNAs in conferring robustness to biological processes. Cell 149, 515–524.

Furukawa, T., Mukherjee, S., Bao, Z.Z., Morrow, E.M., Cepko, C.L., 2000. rax, Hes1, and notch1 promote the formation of Muller glia by postnatal retinal progenitor cells. Neuron 26, 383–394.

Garzon, R., Heaphy, C.E., Havelange, V., Fabbri, M., Volinia, S., Tsao, T., Zanesi, N., Kornblau, S.M., Marcucci, G., Calin, G.A., et al., 2009. MicroRNA 29b functions in acute myeloid leukemia. Blood 114, 5331–5341.

Goldman, D., 2014. Muller glial cell reprogramming and retina regeneration. Nat. Rev. Neurosci. 15, 431–442.

Hackler Jr., L., Wan, J., Swaroop, A., Qian, J., Zack, D.J., 2010. MicroRNA profile of the developing mouse retina. Invest. Ophthalmol. Vis. Sci. 51, 1823–1831.

Huang, D.W.1, Sherman, B.T., Tan, Q., Collins, J.R., Alvord, W.G., Roayaei, J., Stephens, R., Baseler, M.W., Lane, H.C., Lempicki, R.A., 2007. The DAVID Gene Functional Classification Tool: a novel biological module-centric algorithm to functionally analyze large gene lists. Genome Biol. 8 (9), R183.

Iida, A., Shinoe, T., Baba, Y., Mano, H., Watanabe, S., 2011. Dicer plays essential roles for retinal development by regulation of survival and differentiation. Invest. Ophthalmol. Vis. Sci. 52, 3008–3017.

Johnson, R., Teh, C.H., Kunarso, G., Wong, K.Y., Srinivasan, G., Cooper, M.L., Volta, M., Chan, S.S., Lipovich, L., Pollard, S.M., et al., 2008. REST regulates distinct transcriptional networks in embryonic and neural stem cells. PLoS Biol. 6, e256.

Kapinas, K., Kessler, C.B., Delany, A.M., 2009. miR-29 suppression of osteonectin in osteoblasts: regulation during differentiation and by canonical Wnt signaling. J. Cell. Biochem. 108, 216–224.

La Torre, A., Georgi, S., Reh, T.A., 2013. Conserved microRNA pathway regulates developmental timing of retinal neurogenesis. Proc. Natl. Acad. Sci. U. S. A. 110, E2362–E2370.

Levine, E.M., Close, J., Fero, M., Ostrovsky, A., Reh, T.A., 2000. p27(Kip1) regulates cell cycle withdrawal of late multipotent progenitor cells in the mammalian retina. Dev. Biol. 219, 299–314.

Ogawa, M., Saitoh, F., Sudou, N., Sato, F., Fujieda, H., 2017. Cell type-specific effects of p27(KIP1) loss on retinal development. Neural Dev. 12, 17.

Parameswaran, S., Xia, X., Hegde, G., Ahmad, I., 2014 Nov. Hmga2 regulates self-renewal of retinal progenitors. Development 141 (21), 4087–4097. https://doi.org/10.1242/dev.107326.

Rapaport, D.H., Wong, L.L., Wood, E.D., Yasumura, D., LaVail, M.M., 2004. Timing and topography of cell genesis in the rat retina. J. Comp. Neurol. 474, 304–324.

Sherr, C.J., Roberts, J.M., 1995. Inhibitors of mammalian G1 cyclin-dependent kinases. Genes Dev. 9, 1149–1163.

Shin, J., Shin, Y., Oh, S.M., Yang, H., Yu, W.J., Lee, J.P., Huh, S.O., Lee, S.H., Suh, Y.H., Chung, S., et al., 2014. MiR-29b controls fetal mouse neurogenesis by regulating ICAT-mediated Wnt/beta-catenin signaling. Cell Death Dis. 5, e1473.

Ueki, Y., Wilken, M.S., Cox, K.E., Chipman, L.B., Bermingham-McDonogh, O., Reh, T.A., 2015. A transient wave of BMP signaling in the retina is necessary for Muller glial differentiation. Development 142, 533–543.

Wu, H., Sun, S., Tu, K., Gao, Y., Xie, B., Krainer, A.R., Zhu, J., 2010. A splicing-independent function of SF2/ASF in microRNA processing. Mol. Cell 38, 67–77.

Xia, X., Ahmad, I., 2016a. let-7 microRNA regulates neurogliogenesis in the mammalian retina through Hmga2. Dev. Biol. 410, 70–85.

Xia, X., Ahmad, I., 2016b. Unlocking the neurogenic potential of mammalian muller glia. Int. J. Stem Cells 9, 169–175.

Xia, X., Teotia, P., Ahmad, I., 2018. Lin28a regulates neurogliogenesis in mammalian retina through the Igf signaling. Dev. Biol. 440, 113–128.

Young, R.W., 1985. Cell differentiation in the retina of the mouse. Anat. Rec. 212, 199–205.

Zhang, D., Wang, Y., Lu, P., Wang, P., Yuan, X., Yan, J., Cai, C., Chang, C.P., Zheng, D., Wu, B., et al., 2017a. REST regulates the cell cycle for cardiac development and regeneration. Nat. Commun. 8, 1979.

Zhang, Y., Shen, B., Zhang, D., Wang, Y., Tang, Z., Ni, N., Jin, X., Luo, M., Sun, H., Gu, P., 2017b. miR-29a regulates the proliferation and differentiation of retinal progenitors by targeting Rbm8a. Oncotarget 8, 31993–32008.

Zou, H., Ding, Y., Shi, W., Xu, X., Gong, A., Zhang, Z., Liu, J., 2015. MicroRNA-29c/PTEN pathway is involved in mice brain development and modulates neurite outgrowth in PC12 cells. Cell. Mol. Neurobiol. 35, 313–322.